Proceedings of the 2006 IEEE/RSJ
International Conference on Intelligent Robots and Systems
October 9 - 15, 2006, Beijing, China

# Motion Planning of Emergency Stop for Humanoid Robot by State Space Approach

Mitsuharu Morisawa, Kenji Kaneko, Fumio Kanehiro, Shuuji Kajita,
Kiyoshi Fujiwara, Kensuke Harada, Hirohisa Hirukawa
*National Institute of Advanced Industrial Science and Technology(AIST)*
*1-1-1 Umezono, Tsukuba, Ibaraki, 305-8568, Japan*
*Email:{m.morisawa, k.kaneko, f-kanehiro, s.kajita,*
*k-fujiwara, kensuke.harada, hiro.hirukawa }@aist.go.jp*

***Abstract*— A motion planner of emergency stop must make an operating humanoid robot to a stationary state under the emergency signal. It plays an important role in prevention of falling over because humanoid robots fall over easily. Immediately after the emergency signal, it must generate the emergency stop motion in real-time. We modeled a humanoid robot as a simple dynamic system consists of ZMP (Zero-Moment Point) and COG (Center of Gravity) as its states. The emergency stop motion is generated by a state feedback. We determined optimal feedback gains in terms of the initial conditions and the pole assignment. The proposed method realized a reliable emergency stop with low computational cost. Furthermore, it can easily predict the possibility of the successful emergency stop at any time. The validity of the proposed method is confirmed by an experiment using humanoid robot HRP-2.**

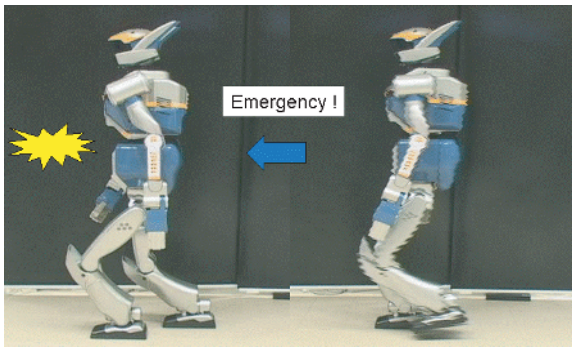


Fig. 1. Emergency stop.

## I. Introduction

Humanoid robots are expected to deal with the complicated tasks in not only the structured environment like industrial manipulator, but also an unstructured environment like human. Especially, since humanoid robots have a high affinity with human, they will assist human in our future. The humanoid robots that have the same size as a human have actively researched and developed [1]-[5]. ASIMO that HONDA R&D Co., Ltd. developed especially achieved a usual walking of 2.7[km/h] and running of 6[km/h], and has physical ability enough for the light labor in such office. However, the biped humanoid robots generally have a fatal weak point. It is easy to fall over because the stability margin is small according to a restriction of support polygon and a high COG position. Therefore, it is necessary to improve the fail-safe technology such as a prevention of falling over before happens like in Fig.1, a control of falling over in case of unavoidableness[6], and a standing by themselves in any state[7] in addition to the walking mobility for working in a living environment. If a human-size humanoid robot falls over, the robot will have suffer physical damage.

As preliminary step toward practical application, the humanoid robots has tried to digitalize the traditional arts or technique such as fork dance and utilize in the entertainment field. Nakaoka[8] et al. achieved Japanese traditional dance with a dynamic whole body motion using HRP-2. Our group developed the biped dinosaur robots and demonstrated in EXPO 2005 Aichi Japan held for 185 days[9]. For long term demonstration, the motion suspension system was introduced in order to ensure safety of spectator and prevent a falling over[10], [11]. This paper proposes the motion planning of emergency stop in motion suspension system. This algorithm forces operating humanoid robot to stop without falling over by emergency stop signal from human operator, or detector of abnormal signals of sensors.

The rest of this paper is organized as follows. The related works about real-time gait planning is overviewed in Section II. The precondition of stop motion is shown in Section III. In Section IV, the details of the motion generation of emergency stop will be explained. How to return home position after emergency stop will be shown in Section V. Experimental results are shown in Section.VI. Finally, we conclude in Section VII.

## II. Related works

Firstly, let us consider the difference between the traditional real-time gait planning and the motion planning of emergency stop. The traditional real-time biped gait can be generated from the preplanned ZMP[12] according to the future footprint. However, the motion planning of emergency stop can not be preplanned because a trigger time from emergency stop signal is unpredictable. At the stop motion, the trajectories of ZMP and COG must be connected to original trajectories continuously and terminal velocity of COG must be 0 explicitly.

Therefore, a motion planning of emergency stop is formulated as an initial and a terminal value mixed problem.

1-4244-0259-X/06/$20.00 ©2006 IEEE

Although the stop motion has to be generated in real-time, the solution of these problems generally needs large calculation cost, because the number of condition is greater than that of unknown parameters. To generate a motion pattern in real-time, the inverted pendulum model which is represented as the linear differential equation is derived by an approximate dynamics of COG[13]-[16]. Kagami[13] realizes a fast generation of dynamically stable humanoid robot walking pattern by digitalizing the differential equation. It is difficult to satisfy the boundary condition of COG in this method. Although the generation method of biped walking pattern by using preview control which is proposed by Kajita[14] can be satisfy the boundary condition, it is difficult to guarantee stable stop motion because it is not clear to relate between the initial value of state variables and the ZMP tracking error. Harada[15] and Sugihara[16] generated a real-time biped gait using an analytical solution. In these methods, the relation to the displacement of ZMP and the initial value is also unclear.

We also proposed the stop motion based on analytical method by optimizing the landing position and time[11]. In this method, the influence of trajectory change of the swing leg can not be negligible and the calculation cost is high with the convergence process. Thus, to improve reliability of the stop motion, we focus on the double support phase and analize the relation of the initial value and the trajectories of ZMP and COG. Then, the stop motion with a high stability margin can be obtained.

## III. Emergency Stop Motion

### A. Preconditions

The preconditions for the motion planning of emergency stop are set as follow,

- The floor is a flat plane.
- The external force is not considered (compensated by stabilization controller).
- The stop motion can only refer to motion pattern (walking parameters are unknown such as walking cycle or velocity).

Here, two kinds of situation for the stop can be considered.

$$\begin{aligned} \text{Static stop} &: \dot{x}(T) = 0 \ \cap \ x(T) = p(T) \\ \text{Dynamic stop} &: \dot{x}(T) = 0 \ \cap \ x(T) \neq p(T) \end{aligned}$$

Where, $T$ is a time when the velocity of COG becomes 0. $x$, and $p$ denote COG and ZMP position respectively. COG can keep the same position as ZMP in the static stop. On the other hand, as for a dynamic stop, because the terminal position of ZMP and COG is different, the acceleration of COG does not become 0. In the next moment, COG will move to an opposite direction and the displacement of ZMP will get larger than of COG. Then, both will be taken to the same position as static stop.

### B. Strategy of emergency stop

In an original operation, stop motion planner just monitors internal states Fig.2 (a). If humanoid robots are put in abnormal circumstances, it will be desirable for robots to take a statically stable posture as soon as possible. Moreover, stop motion must be generated in real-time from any state of robots. The proposed control system is shown in Fig.2. If the joint angular velocity and the differentiation of the ZMP can not be obtained, the stop motion planner always estimates it. When the stop motion planner receives an emergency stop signal, the COG and the ZMP trajectories will be generated according to the internal states at the time. Thus, during the playback of off-line walking pattern, the stop motion planner can be also used to make the walking humanoid robot to stop instantly.

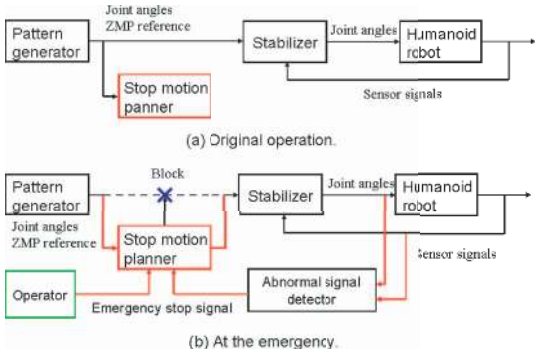


Fig. 2. Signal flow of control system.

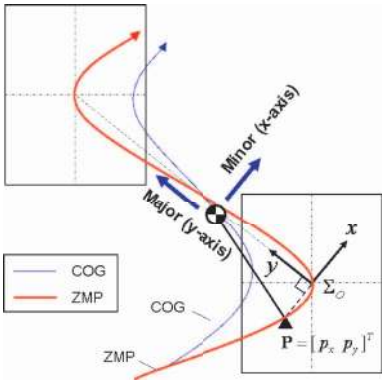


Fig. 3. Coordinate system.

## IV. Motion Planning of Emergency Stop

### A. Coordinate system

A dynamics of humanoid robot can be linearized as a mass system of inverted pendulum with a constant height. Here, let us define a new coordinate system $\sum_o$ which consists of new two axis named Major and Minor axes (Fig.3)[22]. Major axis as $y$ axis is defined in a direction from the center of right foot to the center of the left foot. Minor axis as $x$ axis is defined in an orthogonal direction to Major axis on the floor plane. New origin which is fixed on the ground is defined at the intersection of Major axis and ZMP reference $p_x$ in Minor axis.

Then, motion equation of COG is given as follows.

$$\ddot{\boldsymbol{x}}(t) \quad = \quad \omega_c^2(\boldsymbol{x}(t) - \boldsymbol{p}(t)) \tag{1}$$

Where, $\boldsymbol{x} = [x\ y]^T$ is a vector of horizontal position of COG, $\boldsymbol{p} = [p_x\ p_y]^T$ is ZMP vector projected on the floor plane, $\omega_c$ is natural angular frequency of inverted pendulum, $z_c$ is a height of COG, and $g$ is gravitational constant. Equation (1) can be applied to the horizontal motion in any axis. ZMP is approximated by first order lag system with a cut-off angular frequency $\omega$[21].

$$\dot{\bar{\boldsymbol{p}}}(t) \quad = \quad \omega_f(\boldsymbol{p}(t) - \bar{\boldsymbol{p}}(t)) \tag{2}$$

An approximated ZMP $\bar{\boldsymbol{p}}(t)$ will correspond with an actual ZMP $\boldsymbol{p}(t)$ in a low frequency domain. In this way, the both of ZMP and COG can be represented as the state variables and generable simultaneously.

### B. Motion planning in Minor axis

*1) Derivation of state equation:* The state equation is represented as follows by regarding the acceleration of COG as a system input.

$$\frac{d}{dt}\begin{bmatrix} \bar{p}_x \\ x \\ \dot{x} \end{bmatrix} = \begin{bmatrix} -\omega_f & \omega_f & 0 \\ 0 & 0 & 1 \\ 0 & 0 & 0 \end{bmatrix}\begin{bmatrix} \bar{p}_x \\ x \\ \dot{x} \end{bmatrix} + \begin{bmatrix} -\frac{\omega_f}{\omega_c^2} \\ 0 \\ 1 \end{bmatrix}\ddot{x} \tag{3}$$

This system becomes controllable and can be stabilized by the state feedback control.

$$\ddot{x} = k_{x1}(\bar{p}_x^{ref} - \bar{p}_x) + k_{x2}(x^{ref} - x) + k_{x3}(\dot{x}^{ref} - \dot{x}) \tag{4}$$

The characteristic equation can be given as follows.

$$\begin{aligned} D_x(s) \quad = \quad & s^3 + \left(-\frac{\omega_f}{\omega_c^2}k_{x1} + k_{x3} + \omega_f\right)s^2 \\ & +(k_{x2} + k_{x3}\omega_f)s + (k_{x1} + k_{x2})\omega_f \end{aligned} \tag{5}$$

The margin of stability becomes small in Minor axis on the floor plane. The robot may be caused to fall over by the influence of angular momentum around the COG and the modeling error if ZMP is located in the border of the support polygon. The desired position of ZMP $p_x^{ref}$ is set to origin as the center of the feet. Thus, the trajectory generation in Minor axis can be represented as the initial value problem, and the desired ZMP and COG position will be 0 ($[\bar{p}_x^{ref}\ x^{ref}\ \dot{x}^{ref}]^T = [0\ 0\ 0]^T$). The transfer functions of ZMP $\bar{P}_x(s)$ and COG $X(s)$ are given as follows.

$$\bar{P}_x(s) \quad = \quad \frac{C_{x1}(s)\bar{P}_x(0) + C_{x2}(s)X(0) + C_{x3}(s)\dot{X}(0)}{D_x(s)} \tag{6}$$

$$X(s) \quad = \quad \frac{C_{x4}(s)\bar{P}_x(0) + C_{x5}(s)X(0) + C_{x6}(s)\dot{X}(0)}{D_x(s)} \tag{7}$$

Where,

$$\begin{aligned} C_{x1}(s) &= s^2 + k_{x3}s + k_{x2}, \\ C_{x2}(s) &= \left(\frac{\omega_f k_{x2}}{\omega_c^2} + \omega_f\right)s + k_{x3}\omega_f, \\ C_{x3}(s) &= \frac{\omega_f k_{x3}}{\omega_c^2}s + \frac{\omega_f k_{x2}}{\omega_c^2} + \omega_f, \\ C_{x4}(s) &= k_{x1}, \\ C_{x5}(s) &= s^2 + \left(\frac{\omega_f k_{x1}}{\omega_c^2} - k_{x3} - \omega_f\right)s + k_{x3}\omega_f, \\ C_{x6}(s) &= s - \frac{\omega_f k_{x1}}{\omega_c^2} + \omega_f. \end{aligned}$$

*2) Design of control system:* The inverted pendulum generally has a specific characteristic of non-minimum shift phase. In such system, it is known that the tracking performance has a limitation by any feedback control[20]. However, in term of the initial value problem for the position of ZMP and COG in (6) and (7), it is possible to generate the trajectories of ZMP and COG with an undershootless or an overshootless by the suitable feedback gain, because there is no unstable zero point at the numerator. The system matrix includes the COG height which value can not be determined until the emergency signal is given. Thus, the feedback gain will be calculated online by the pole placement method. The poles refer to the value in which the feedback gain calculated with the optimal regulator is converted into the pole. Figure 4 shows the time response of ZMP and COG in Minor axis actually generated at each walking speed. An initial value of ZMP and COG used the

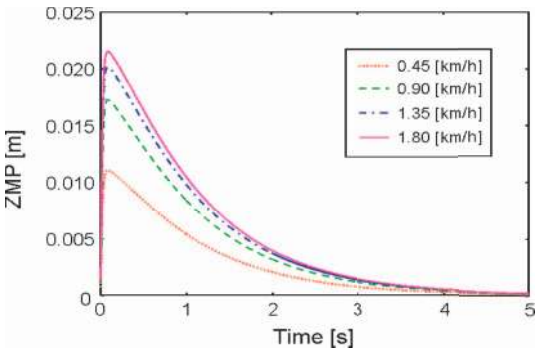


Fig. 4. Time responses of ZMP and COG at minor axis.

value at the beginning of double support phase after the fifth step. The displacement of maximum ZMP which is less than 0.022[m] at 1.8[km/h], is small for the support polygon of HRP-2. Although the support polygon in Minor axis becomes smaller with getting longer for a step length, the amplitude of ZMP is enough little.

### C. Motion planning in Major axis

*1) Derivation of state equation:* The margin of stability becomes relatively large in Minor axis defined in a direction from the center of left foot to the center of the right foot. COG in Major axis has some degree of velocity at the beginning of double support phase. The overshoot is caused if the desired

ZMP is not appropriately given. Thus, the relative position of ZMP and COG is derived as a new state variable.

$$r(t) = y(t) - \bar{p}_y(t) \tag{8}$$

From (3) and (8), the degenerate state equation can be obtained.

$$\frac{d}{dt}\begin{bmatrix} r \\ \dot{y} \end{bmatrix} = \begin{bmatrix} -\omega_f & 1 \\ 0 & 0 \end{bmatrix}\begin{bmatrix} r \\ \dot{y} \end{bmatrix} + \begin{bmatrix} \frac{\omega_f}{\omega_c^2} \\ 1 \end{bmatrix}\ddot{y} \tag{9}$$

Each position, ZMP and COG can be calculated by integrating the velocity of COG and the relative position of ZMP and COG in (9).

$$y(t) = \int_{t_0}^{t} \dot{y}(\tau)d\tau, \tag{10}$$

$$\bar{p}_y(t) = y(t) - r(t) - \bar{p}_y(t_0). \tag{11}$$

This system also will be controllable and can be stabilized by state feedback controller.

$$\ddot{y} = -k_{y1}r - k_{y2}\dot{y} \tag{12}$$

The characteristic equation of this system $D_y(s)$ can be given as follows.

$$D_y(s) = s^2 + \left(\omega_f + \frac{\omega_f k_{y1}}{\omega_c^2} + k_{y2}\right)s + k_{y1} + k_{y2}\omega_f \tag{13}$$

Origin is defined in the desired ZMP position at the beginning of double support phase. In this way, a motion planning in Major axis can be also formulated as the initial value problem as well as in Minor axis, because the desired value of all of state variables will be 0. Then, the transfer function of ZMP and COG can be obtained by setting the initial value of COG to $Y(0)$ and $\dot{Y}(0)$,

$$\bar{P}_y(s) = \frac{C_{y1}(s)Y(0) + C_{y2}(s)\dot{Y}(0)}{H(s)}, \tag{14}$$

$$Y(s) = \frac{C_{y3}(s)Y(0) + C_{y4}(s)\dot{Y}(0)}{H(s)}, \tag{15}$$

where,

$$\begin{aligned} C_{y1}(s) &= \left(\frac{\omega_f k_{y1}}{\omega_c^2} + \omega_f\right)s + k_{y2}\omega_f, \\ C_{y2}(s) &= \frac{\omega_f k_{y2}}{\omega_c^2}s + \frac{\omega_f k_{y1}}{\omega_c^2} + \omega_f, \\ C_{y3}(s) &= s^2 + \left(\frac{\omega_f k_{y1}}{\omega_c^2} + \omega_f + k_{y2}\right)s + k_{y2}\omega_f, \\ C_{y4}(s) &= s + \frac{\omega_f k_{y1}}{\omega_c^2} + \omega_f, \\ H(s) &= sD_y(s) \end{aligned}$$

*2) Design of control system:* The feedback gain taking each maximum displacement of ZMP and COG into account can not be calculated by a typical optimal regulator, because the evaluate function including the integration of the velocity of COG is diverged. In this paper, the feedback gain will be calculated by the relation between the maximum displacement of ZMP and the roots of the characteristic equation.

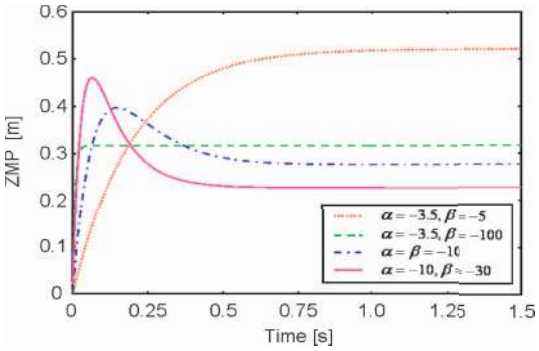


Fig. 5. Transient responses of ZMP (1.35[km/h]).

The response of ZMP can be obtained by inverse Laplace transform,

$$\bar{p}_y(t) = \mathscr{L}^{-1}[\bar{P}_y(s)] = n_1 e^{\alpha t} + n_2 e^{\beta t} + n_3, \tag{16}$$

where $\alpha, \beta$ denote the roots of the characteristic equation in (13). The coefficients of (16) imply as follows.

$$n_1 = \frac{\left(\alpha^2 - \omega_c^2\right)\left(-\left(1 + \frac{\beta}{\omega_f}\right)y_0 + \left(\frac{\beta}{\omega_c^2} + \frac{1}{\omega_f}\right)\dot{y}_0\right)}{\left(1 - \frac{\omega_c^2}{\omega_f^2}\right)(\alpha - \beta)\alpha}$$

$$n_2 = \frac{\left(\beta^2 - \omega_c^2\right)\left(-\left(1 + \frac{\alpha}{\omega_f}\right)y_0 + \left(\frac{\alpha}{\omega_c^2} + \frac{1}{\omega_f}\right)\dot{y}_0\right)}{\left(1 - \frac{\omega_c^2}{\omega_f^2}\right)(\beta - \alpha)\beta}$$

$$n_3 = \frac{\left(\omega_c^2\left(1 + \frac{\alpha+\beta}{\omega_f}\right) + \alpha\beta\right)y_0 - \left(\alpha + \beta + \frac{\omega_c^2 + \alpha\beta}{\omega_f}\right)\dot{y}_0}{\left(1 - \frac{\omega_c^2}{\omega_f^2}\right)\alpha\beta}$$

As the roots of the characteristic equation are satisfied by

$$\alpha = -\omega_c,\ \beta < -\omega_c, \tag{17}$$

the coefficients can be always comprised as follows.

$$n_1 = 0,\ n_2 < 0 \tag{18}$$

The transient response can be avoided the undershoot or the overshoot at any given the initial position and velocity of COG. Figure 5 shows the difference of the response corresponding to the pole placement.

As $\alpha$ is approached to the natural angular frequency of inverted pendulum ($= \omega_c$) and $\beta$ is located on the far from the origin, the smaller maximum ZMP can be obtained and shown in Fig.6. Thus, the feedback gain can be calculated by the roots of the characteristic equation.

$$k_{y1} = \frac{-\omega_c^2\left(1 + \frac{\alpha+\beta}{\omega_f} + \frac{\alpha\beta}{\omega_f^2}\right)}{\left(1 - \frac{\omega_c^2}{\omega_f^2}\right)} \tag{19}$$

$$k_{y2} = \frac{\frac{\omega_c^2(\alpha+\beta)}{\omega_f^2} + \frac{\omega_c^2 + \alpha\beta}{\omega_f}}{\left(1 - \frac{\omega_c^2}{\omega_f^2}\right)} \tag{20}$$

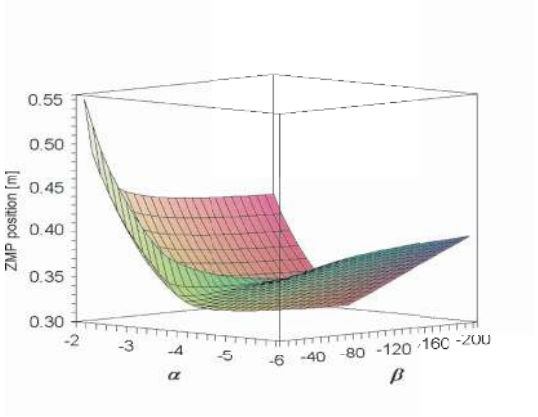


Fig. 6. Maximum ZMP according to pole location (1.35[km/h]) .

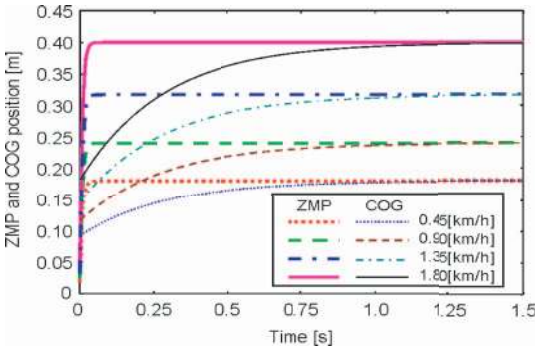


Fig. 7. Time responses of ZMP and COG at major axis ($\alpha = -3.5, \beta = -100$).

Figure 7 shows the time responses of ZMP and COG at each walking speed under $\alpha = -3.5, \beta = -100$. The maximum displacement of ZMP and COG increases mostly in proportion to the walking speed. The maximum displacement of ZMP will be equal to the terminal position of ZMP and COG, that is

$$\begin{aligned} \bar{p}_{y,max} &= y_{max} \\ &= \lim_{t\to\infty} \bar{p}_y(t) \\ &= n_3. \end{aligned} \tag{21}$$

Thus, it is possible to check whether a stable stop can be realized and the leg joints can move within the working area from the maximum position of ZMP and COG before the beginning of the emergency stop motion. Figure 8 shows the relation between walking speed and the maximum displacement of COG at 0.8[s] step cycle. The motion of COG in the frontal plane has a large influence on the motion of COG in the direction of Major axis when the walking speed is slow. The maximum displacement of COG will remain within the center of feet with the suitable feedback gain. The knee joint is stretched beyond the limits of the movable area at a walking speed greater than the 1.8[km/h]. In such case, the waist is required to crouch down according to the movable limitation.

The trajectory of ZMP approaches the step response as $\beta$ is set far from the origin. On the assumption that a cut-off frequency of approximated ZMP is enough high ($\omega_f \to \infty$),

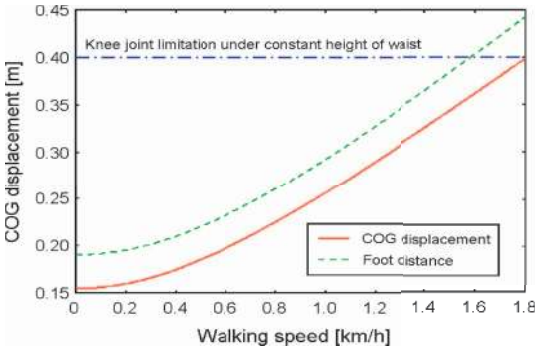


Fig. 8. COG displacement.

the minimum value of actual ZMP can be given as follows.

$$\begin{aligned} p_{y,min} &= \lim_{\beta\to-\infty} \left( \sup_{t=[0:\infty)} \| p_y(t) \| \right) \\ &= y_0 + \frac{\dot{y}_0}{\omega_c} \end{aligned} \tag{22}$$

This is equivalent to make a mass of inverted pendulum to stop on the support point by actuating the support point instantaneously. In fact, it is desirable to set the poles according to the ZMP tracking performance of the stabilization controller. Moreover, the influence of angular momentum around COG was negligible small in mostly cases even if the robot behave dynamically. Finally, an actual motion of COG can be obtained from the generated COG motion in Major and Minor axes by the inverse coordinate transformation.

## V. Return Motion to Home Position

A whole body motion is not uniquely determined only by the motion planning of COG. The motion of COG can be achieved by the motion in the horizontal direction of the waist. The rest of degree of freedom are planned in joint space.

$$\theta(t) = \theta_0 + \dot{\theta}_0 t - \frac{\dot{\theta}_0}{T_b} t^2 + \frac{\dot{\theta}_0}{3T_b^2} t^3. \tag{23}$$

The stop time $T_b$ is given so that the angle of joints after stop can not go over a workspace. After the emergency stop, it can return to the home position by the following sequences.

1) Stop all of joints
2) Move upper joints to home position
3) Align the feet by stepping

## VI. Experiment

The validity of the proposed method is shown using humanoid robot HRP-2. The straight walking at the walking speed of 2.5[km/h] was tested. Double support phase was detected by the relative height of feet calculated from the joint angles of legs and the reference of the waist position and attitude.

The trajectories of ZMP and COG in frontal and sagittal plane which was synthesized from the trajectories in Major and in Minor axes are shown in Fig.10 (a) and (b). Figure 10

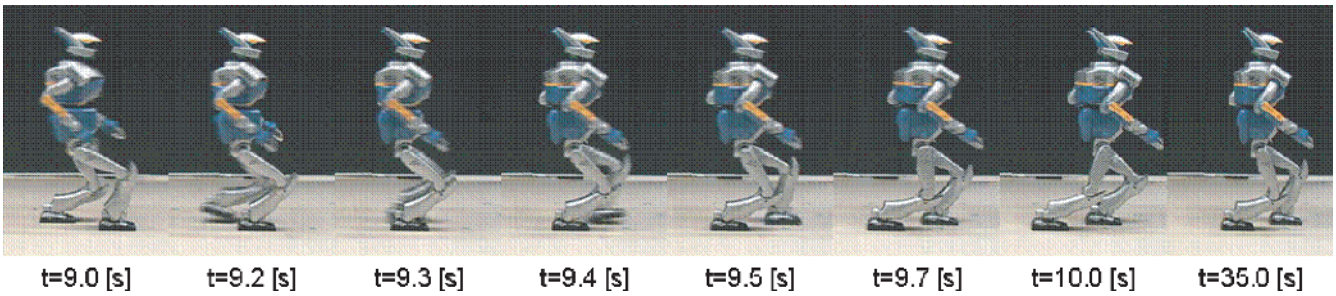


Fig. 9. Snapshot of emergency stop

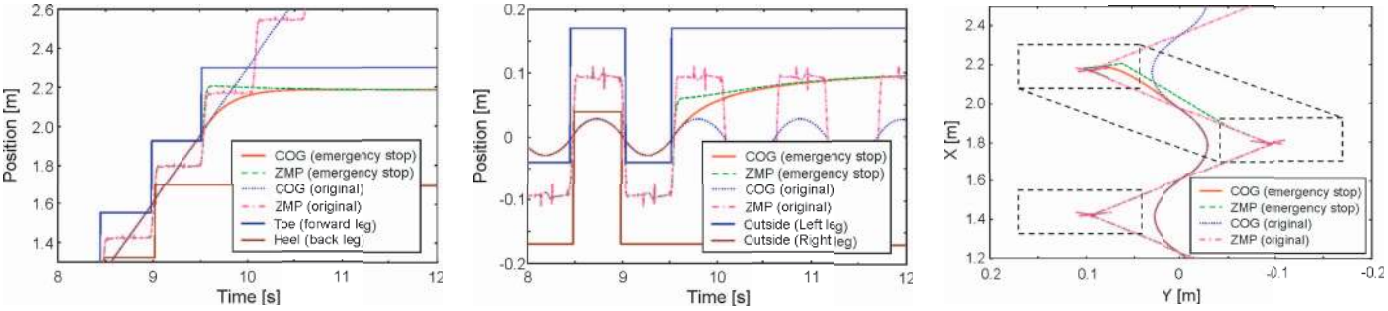


(a) Sagittal plane. (b) Frontal plane. (c) Projection on the floor.

Fig. 10. ZMP and COG trajectories

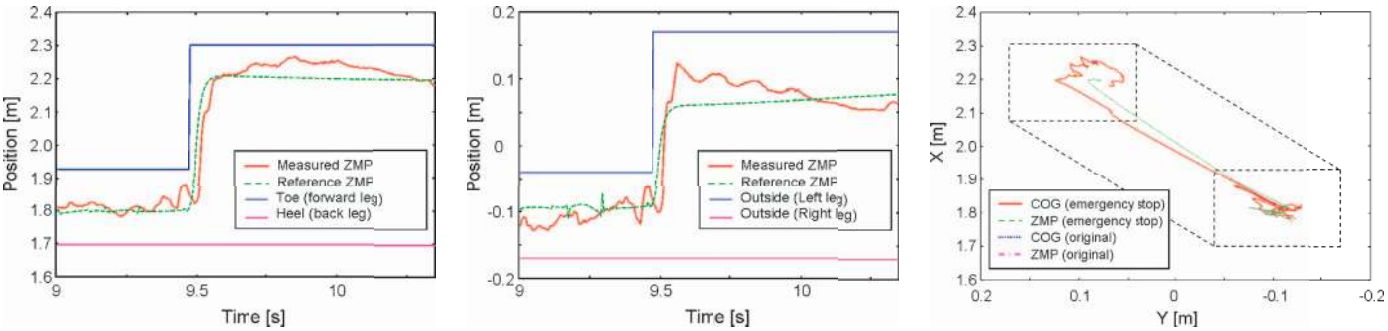


(a) Sagittal plane. (b) Frontal plane. (b) Projection on the floor.

Fig. 11. ZMP response

(c) shows the locus of ZMP and COG projected to the floor plane. Actual ZMP responses in frontal and sagittal plane are shown in 11. The snapshot of the emergency stop is shown in Fig.9. The stop motion started at 9.5[s]. There is an enough stability margin in the emergency stop at the walking speed of 2.5[km/h]. In a sequence of motion, the waist had crouched down so that the knee joint can not be stretched, because the horizontal motion of COG was large.

## VII. Conclusion

In this paper, the motion generation algorithm of emergency stop for a humanoid robot was proposed. The trajectories of ZMP and COG, which were introduced as the state variables, could be generated simultaneously by a simple rule of state feedback. Then, the suitable feedback gains were determined in relation to the displacement of ZMP and COG and poles of a state space system. The advantages of the proposed method were,

- The high reliability for the emergency stop was ensured by analyzing the maximum displacement of ZMP and COG.
- Calculation cost of motion planning is very small by using state space approach.

Thus, it was succeeded to check whether the robot can stop or not before starting the stop motion. The validity of the proposed method was confirmed by experiment using humanoid robot HRP-2. The emergency stop in uneven terrain is our challenge.

## REFERENCES


[1] K.Hirai, et al., "The Development of Honda Humanoid Robot," Proc. of IEEE Int. Conf. on Robotics and Automation, pp.1321-1326, 1998.

[2] Y.Kuroki, et al., "A Small Biped Entertainment Robot Exploring Attractive Applications," Proc. of IEEE Int. Conf. on Robotics and Automation, pp.471-476, 2001.

[3] M.Gienger, et al., "Towards the Design of Jogging Robot," Proc. of IEEE Int. Conf. on Robotics and Automation, pp.4140-4145, 2001.

[4] J.Y.Kim, et al., "System Design and Dynamic Walking of Humanoid Robot KHR-2," Proc. of IEEE Int. Conf. on Robotics and Automation, pp.1443-1448, 2005.

[5] K.Kaneko, et al., "The Humanoid Robot HRP2," Proc. of IEEE Int. Conf. on Robotics and Automation, pp.1083-1090, 2004.

[6] K.Fujiwara, et al.,"The First Human-size Humanoid that can Fall Over Safely and Stand-up Again," Proc. of IEEE/RSJ Int. Conf. on IROS, pp.1920-1926, 2003

[7] F.Kanehiro, "The First Humanoid Robot that Has the Same Size as a Human and that Can Lie down and Get up," Proc. of IEEE Int. Conf. on Robotics and Automation, pp.1633-1639, 2003.

[8] S.Nakaoka, et al.,"Task Model of Lower Body Motion for a Biped Humanoid Robot to Imitate Human Dances," Proc. of IEEE/RSJ Int. Conf. on IROS, pp.2769-2775, 2005.

[9] K.Kaneko, at el, "Bipedal Dinosaur Robot," Proc. of the 23th Annual Conf. on RSJ, CD-ROM, 2G17, 2005 (in Japanese)

[10] K.Kaneko, at el, "Motion Suspension System for Humanoids," Proc. of the 23th Annual Conf. on RSJ, CD-ROM, 2F21, 2005. (in Japanese)

[11] M.Morisawa, et al., "Emergency Stop Algorithm for Walking Humanoid Robots," Proc. of IEEE/RSJ Int. Conf. on IROS, pp.31-37, 2005.

[12] M.Vukobratovic, and D.Juricic, "Contribution to the Synthiesis of Biped Gait," IEEE Trans. on Bio-Med. Eng., vol.BME-16, no.1, pp.1-6,1969.

[13] S.Kagami, at el., "A Fast Generation Method of a Dynamically Stable Humanoid Robot Trajectory with Enhanced ZMP Constraint," Proc. of the 2000 IEEE-RAS Int. Conf. Humanoid Robots, 2000.

[14] S.Kajita, et al., "Biped Walking Pattern Generation by using Preview Control of Zero-Moment Point," Proc. of IEEE Int. Conf. on Robotics and Automation, pp.1620-1626, 2003.

[15] K.Harada, et al., "An Analytical Method on Real-time Gait Planning for a Humanoid Robot," Proc. of the 2000 IEEE-RAS Int. Conf. Humanoid Robots, Paper #60, 2004.

[16] T.Sugihara, et al., "A Fast Online Gait Planning with Boundary Condition Relaxation for Humanoid Robot," Proc. of IEEE Int. Conf. on Robotics and Automation, pp.306-311, 2005.

[17] Y.Okumura, et al, "Realtime ZMP Compensation for Biped Walking Robot using Adaptive Inertia Force Control," Proc. of IEEE/RSJ Int. Conf. on IROS, pp.335-339, 2003.

[18] T.Sugihara, Y.Nakamura, H.Inoue, "Realtime Humanoid Motion Generation through ZMP Manipulation based on Inverted Pendulum Control," Proc. of IEEE Int. Conf. on Robotics and Automation, pp.1404-1409, 2002.

[19] S.Kajita, et al., "The 3D Linear Inverted Pendulum Mode: A simple modeling for a biped walking pattern generation," Proc. of IEEE/RSJ Int. Conf. on IROS, pp.239-246, 2001.

[20] Napoleon, et al.,"Balance Control Analysis of Humanoid Robot based on ZMP Feedback Control," Proc. of IEEE/RSJ Int. Conf. on IROS, pp.2437-2442, 2002

[21] S.Kajita, "Humanoid Robots", Ohmusha, ISBN4-274-20058-2, 2005. (in Japanese)

[22] K.Kaneko et al., Japanese PAT.3646169 (in Japanese).